CD44 EXPRESSION DYNAMICS IN THE CORPUS CALLOSUM AFTER CUPRIZONE-INDUCED DEMYELINATION

L. Gaydarski[1], K. Petrova[1], G.P. Georgiev[2], B. Landzhov[1]

[1]Department of Anatomy, Histology and Embryology, Medical University – Sofia, Bulgaria
[2]Department of Orthopedics and Traumatology, University Hospital "Tsaritsa Yoanna -ISUL", Medical University – Sofia, Bulgaria

Abstract. Background: *CD44, a hyaluronan receptor expressed by glial and progenitor cells, has been implicated in neuroinflammation and impaired remyelination. We investigated changes in CD44 expression and cell morphology in the corpus callosum (CC) during toxin-induced demyelination and subsequent spontaneous remyelination.* **Materials and Methods:** *Thirty adult male C57BL/6 mice were assigned to three groups (n = 10/ group): control, demyelination (0.2% cuprizone for 5 weeks), and remyelination (5 weeks of cuprizone followed by 5 weeks of recovery). CD44 immunohistochemistry was performed on coronal CC sections. Quantification was carried out in the medial CC (three sections per animal, five non-overlapping fields per section; total n = 150 visual fields per group). Morphological features of CD44+ cells were assessed qualitatively. Group differences were analyzed using the Kruskal–Wallis test with Dunn's post-hoc comparisons.* **Results:** *In the controls, CD44 immunoreactivity was sparse and primarily localized to the perinuclear region. Demyelination resulted in a marked increase in CD44 labeling, with CD44+ cells being substantially more numerous and exhibiting multiple cytoplasmic processes consistent with an activated astrocytic phenotype. During remyelination, CD44 labeling persisted but with fewer and shorter processes, indicating partial reversion toward a less activated morphology. Mean CD44+ cells per field were 19 (control), 57 (demyelination), and 32 (remyelination), corresponding to densities of 183, 528, and 426 cells/mm², respectively (control < remyelination < demyelination). Differences among groups were significant (Kruskal–Wallis, p < 0.001), and all pairwise comparisons were significant (Dunn's test, p < 0.001).* **Conclusions:** *Cuprizone-induced demyelination triggers robust upregulation of CD44 and an activated astrocyte–like morphology in the CC, which partially normalizes during remyelination. These results highlight the dynamic regulation of CD44 during white matter injury and recovery and support further investigation into its mechanistic role in remyelination.*

Corresponding author: Lyubomir Gaydarski, MD, Department of Anatomy, Histology and Embryology, Medical University – Sofia, 2 Zdrave str, Sofia 1431, Bulgaria, tel: +359885037178, email: lgaidarsky@gmail.com

ORCID: 0000-0003-4774-6507

INTRODUCTION

Multiple sclerosis (MS) is a chronic autoimmune disorder characterized by T-lymphocyte infiltration into the central nervous system (CNS), leading to demyelination and impaired nerve conduction [1-3]. To investigate the cellular and molecular mechanisms underlying myelin damage and repair independently of peripheral immune influences, the cuprizone mouse model is widely used. In this model, oligodendrocytes are selectively injured through metabolic and oxidative stress, resulting in highly reproducible demyelination within a defined time window and subsequent remyelination upon toxin withdrawal. Because cuprizone primarily affects the CNS and involves minimal peripheral immune activation, it provides a powerful tool for studying intrinsic mechanisms of oligodendrocyte injury and recovery [4].

CD44 is a transmembrane glycoprotein that functions as a principal receptor for hyaluronic acid (HA) and plays a key role in cell adhesion, migration, and inflammatory signaling [5]. CD44 promotes the uptake and clearance of HA, thereby contributing to the resolution of tissue damage signals and inflammation [6]. CD44 exists in multiple isoforms with distinct roles in the CNS. The standard form, CD44s, which lacks variable exons, is the most abundant and is predominantly expressed on astrocytes and oligodendrocyte precursor cells (OPCs) [7]. In contrast, the variant isoforms, CD44v, contain variable exons and are more commonly linked to pathological conditions, such as cancer and active immune responses, but they are less prevalent in the CNS compared with CD44s [8]. Although CD44 is expressed by both immune cells and CNS-resident cells, its expression in the healthy brain is relatively low and becomes markedly upregulated under pathological conditions [9]. In MS, elevated levels of CD44 and HA facilitate immune cell infiltration into the CNS and interfere with oligodendrocyte progenitor cell maturation, thereby limiting remyelination [10].

Beyond its role in inflammation, CD44 is dynamically regulated during neural development and repair. It is initially expressed in neural stem and progenitor cells and subsequently changes as these cells differentiate into neurons and astrocytes [11]. Following cerebral ischemia, ischemia-induced stem cells express CD44 and retain the capacity to differentiate into multiple neural lineages, including microglia-like cells that contribute to the regulation of stem cell niches, suggesting that CD44 marks both progenitor cells and their local microenvironment in the injured brain [12]. In line with these findings, Reinbach et al.

reported increased CD44 expression in the corpus callosum (CC) of cuprizone-treated mice [13]. Moreover, genetic loss of CD44 results in reduced regulatory T-cell numbers, a shift toward proinflammatory T-cell responses, and increased permeability of the blood–brain barrier even under baseline conditions, revealing a previously unrecognized role for CD44 in maintaining vascular integrity beyond autoimmune pathology [14].

Taken together, these observations indicate that CD44 is positioned at the intersection of immune regulation, neural progenitor biology, and tissue repair in the CNS. Therefore, in the present study, we examine the number and distribution of CD44-positive cells in the CNS during cuprizone-induced demyelination and remyelination in order to better define their contribution to myelin pathology and repair.

MATERIALS AND METHODS

Thirty male C57BL/6 mice (8 weeks old) were obtained from the vivarium of the Faculty of Medicine, Medical University – Sofia, Bulgaria, and randomly assigned to three experimental cohorts (n = 10 per group): a control group receiving a standard diet, a demyelination group fed a diet containing 0.2% cuprizone for 5 weeks, and a remyelination group that received the same 5-week 0.2% cuprizone regimen, followed by a 5-week recovery period on standard chow without cuprizone. Animals were housed under standardized environmental conditions (ambient temperature 22 ± 3 °C, relative humidity ≈30%) on a 12-h light/12-h dark cycle, and all experimental procedures were performed during the light phase. All interventions conformed to Directive 2010/63/EU on the protection of animals used for scientific purposes and were approved by the Bulgarian Food Safety Agency (Approval Protocol No. 416/19.12.2024).

Demyelination was induced in 8-week-old C57BL/6 mice by a five-week exposure to the copper chelator cuprizone, using the well-established cuprizone model [4,15]. Cuprizone (CAS 370-81-0; Sigma-Aldrich, Vienna, Austria) was delivered ad libitum in the animals' drinking water at a concentration of 0.2% (w/v). After the five-week treatment period, cuprizone was removed, and mice were maintained on plain drinking water for an additional five weeks to allow spontaneous remyelination. Control animals received only unmodified drinking water for the entire duration of the experiment.

Animals were anesthetized by intraperitoneal injection of thiopental sodium (30 mg/kg; Sigma-Aldrich Chemie GmbH, Taufkirchen, Germany) and then perfused transcardially with 4% paraformaldehyde

in 0.1 M phosphate-buffered saline (pH 7.4; Merck Catalogue No. 1465920006). Brains (n = 30; 10 per experimental group) were removed and post-fixed in the same fixative for 24 hours. Following fixation, tissues were washed, processed through graded dehydration and cleared, and embedded in paraffin blocks (Merck Catalogue No. 1071511000). Serial coronal sections (6 µm) spanning bregma +0.98 to +0.02, as defined in the Mouse Brain Atlas of Paxinos and Franklin [16], were cut on a Leica RM 2155 microtome (Wetzlar, Germany).

Slides were deparaffinized in three changes of xylene (Merck Cat. No. 1082984000), 10 minutes per change, then rehydrated through a graded ethanol series (100%, 95%, 90%, 80%, 70% — Merck Cat. No. 1009835000) and rinsed in distilled water for 5 minutes at each step. Antigen retrieval was performed by heating the sections at 95 °C for 20 minutes in Citrate Plus (10×) HIER Solution (pH 6.0; ScyTek Cat. No. CPL500). After cooling, slides were washed three times (5 min each) in Tris-buffered saline containing 0.05% Tween-20 (TTBS; E-BC-R335, Wuhan Elabscience), and endogenous peroxidase activity was quenched with 3% hydrogen peroxide in distilled water for 10 minutes, followed by three additional TTBS washes (5 min each). Non-specific binding was minimized by incubating the sections with Super Block (ScyTek) for 5 minutes at room temperature. Endogenous biotin was neutralized using the ScyTek biotin-blocking *kit* (BBK120) according to the manufacturer's protocol (15 minutes with reagent A, wash, then 15 minutes with reagent B). To prevent cross-reactivity with mouse immunoglobulins, a mouse-to-mouse blocking reagent (ScyTek Cat. No. MTM015) was applied for 1 hour at room temperature. After a brief TTBS wash, sections were incubated overnight at 4 °C with primary antibody against CD44 (mouse monoclonal, SC-9960, Santa Cruz Biotechnology) diluted 1:200. Immunodetection was carried out using the UltraTek HRP Anti-Polyvalent staining system (ScyTek Cat. No. AFN600) per the supplier's instructions. Finally, sections were counterstained with hematoxylin, dehydrated through ascending ethanols, cleared in xylene, and coverslipped. Negative controls were processed in parallel with the primary antibody replaced by antibody diluent.

Statistical analyses and figure generation were performed using GraphPad Prism 10.6.1 and IBM SPSS Statistics v28.0.0.1. Group comparisons were carried out using the Kruskal-Wallis test, and post-hoc Dunn's test with p ≤ 0.05 was considered statistically significant. Sample sizes comprised ten animals per experimental group; from each group, three slides were prepared, and five non-overlapping microscopic

fields per slide were assessed (total fields n = 150) to enumerate CD44+ cells according to the counting procedure described by our previous study [15].

RESULTS

Immunohistochemical analysis of CD44 was performed on 150 visual fields per group in the medial CC. The region of interest (ROI) is indicated in Fig. 1, which was adapted from the mouse brain atlas of Paxinos and Franklin [16].
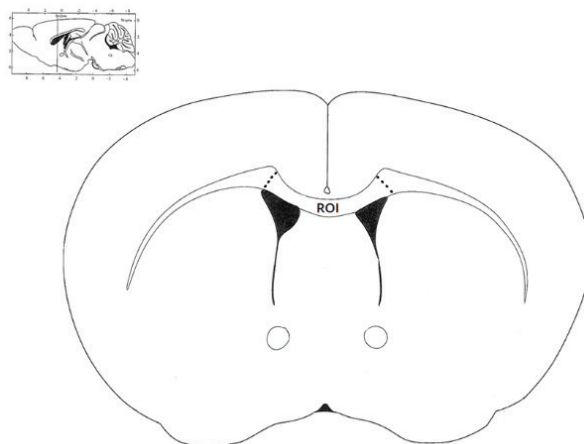

Fig. 1. Schematic representation of the region of interest (ROI) in the medial corpus callosum (CC) of the mouse brain used for CD44 immunohistochemistry and quantification. The ROI is outlined with a dashed line. The figure is adapted from the mouse brain atlas of Paxinos and Franklin [16]

The IHC analysis revealed distinct morphological and quantitative differences among the examined groups in the medial CC. In the control group, CD44 immunoreactivity was very scarce and restricted mainly to the perinuclear cytoplasmic domain of cells. In contrast, the demyelination group showed a marked increase in CD44 expression, with well-defined labeling of cells exhibiting numerous cytoplasmic processes, consistent with an activated astrocytic phenotype. In the remyelination group, CD44 immunoreactivity remained clearly visible; however, the labeled cells displayed fewer cytoplasmic processes, suggesting a transition from an activated toward a less activated astrocytic state. Quantitative analysis performed in the medial CC demonstrated a clear increase in the number of CD44-positive cells during demyelination and a partial reduction during remyelination. The mean number of CD44-positive cells per field was 19 in the control group, 57 in the demyelination group, and 32 in the remyelination group, corresponding to densities of 183 cells/mm², 528 cells/mm², and 426 cells/mm², respectively, following the pattern control < remyelination < demyelination. Statistical analysis

confirmed that these differences among groups were significant (Kruskal–Wallis, p < 0.001), and all post-hoc pairwise comparisons were also significant (p < 0.001), indicating robust group-dependent changes in CD44 expression associated with demyelination and partial normalization during remyelination, as demonstrated in Fig. 2.

DISCUSSION

In this study, we quantified CD44-positive cells in the medial CC of cuprizone-fed C57BL/6 mice during demyelination and remyelination. We observed that CD44+ cell numbers were highest during peak demyelination, lowest in controls, and intermediate during remyelination. Our findings indicate that CD44 upregulation is dynamically regulated in response to oligodendrocyte injury and suggest a reactive glial response to white matter damage. CD44 is widely expressed in the CNS, with glial cells showing increased expression in both animal models and patients with MS, whereas oligodendrocytes in vitro exhibit significantly increased receptor levels under pathological conditions compared with astrocytes [10]. Functionally, elevated CD44 in demyelinated lesions may impair remyelination by promoting the accumulation of high-molecular-weight hyaluronan, which reversibly blocks OPC maturation and inhibits myelin repair [10]. These observations in the EAE model are consistent with our results in the cuprizone model, supporting the concept that CD44 contributes to local regulation of glial and progenitor cell activity in demyelinated lesions.

CD44+ cells in the CNS are considered precursor populations, including astrocytes, oligodendrocytes, and neural progenitors, as demonstrated by Naruse et al. in the developing cerebellum [11]. During development, CD44 expression is initially broad in neural stem and progenitor cells but becomes restricted to specific glial and neuronal populations in a stage-dependent manner. Its expression is transient in oligodendrocyte precursors and immature astrocytes, maintained in fibrous astrocytes and maturing neurons, and downregulated upon terminal differentiation [12]. This developmental pattern suggests that
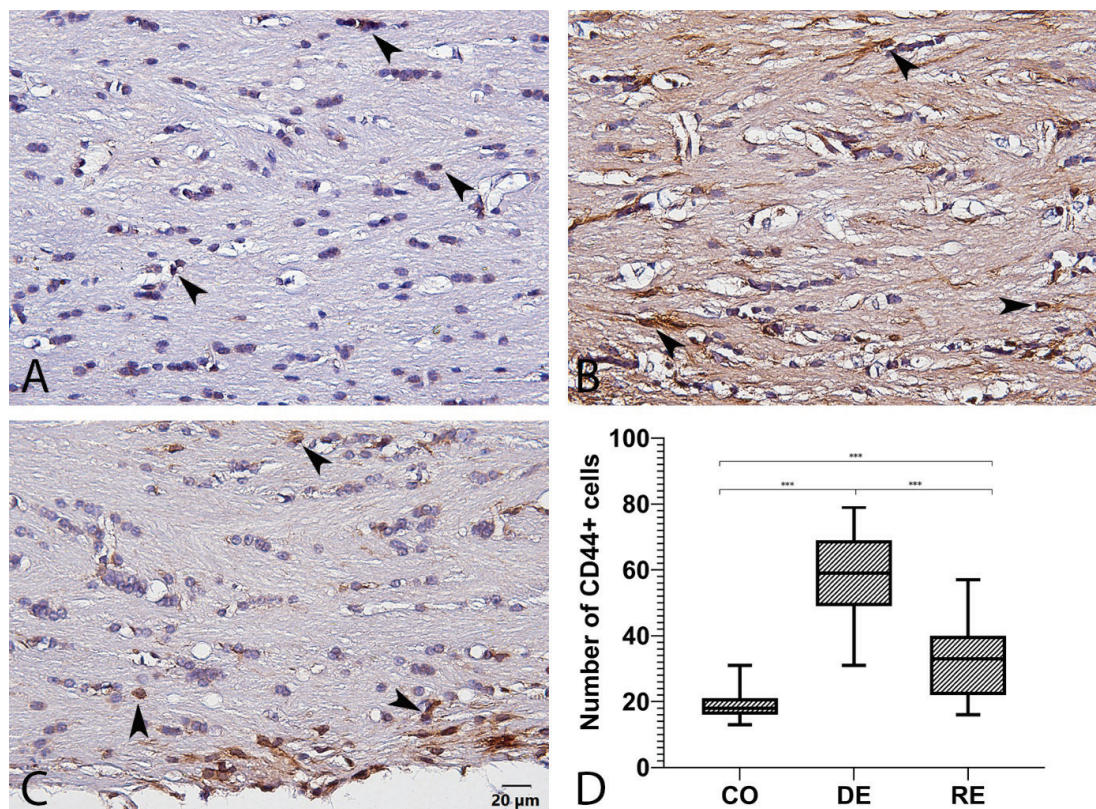

Fig. 2. CD44 immunoreactivity in the medial corpus callosum (CC) across experimental groups. (**A**) Control group showing scarce CD44 immunoreactivity, mainly confined to perinuclear cytoplasmic domains (arrowheads). (**B**) Demyelination group demonstrating markedly increased CD44 immunoreactivity with numerous CD44-positive cells exhibiting multiple cytoplasmic processes (arrowheads). (**C**) Remyelination group showing persistent but reduced CD44 immunoreactivity compared with demyelination, with CD44-positive cells displaying fewer cytoplasmic processes (arrowheads). Scale bar: 20 μm. (**D**) Box-and-whisker plot illustrating the number of CD44-positive cells in the CC across groups (CO, control; DE, demyelination; RE, remyelination). Boxes represent the interquartile range with the median indicated, and whiskers denote the minimum and maximum values. Statistical significance between groups is indicated (*** p < 0.001)

CD44 serves as a marker of cellular plasticity and proliferative potential, which may be reactivated during CNS injury, aligning with our results of increased CD44+ cells in demyelinating lesions in the CC.

Comparisons across demyelination models reveal context-dependent roles of CD44. In MOG-induced EAE, CD44 has a protective, immunoregulatory role by limiting Th17-driven inflammation, maintaining regulatory T-cell populations, and preserving blood–brain barrier integrity. CD44 deficiency exacerbates immune cell infiltration, vascular permeability, and demyelination, resulting in more severe neurological deficits [14]. In contrast, in cuprizone-induced demyelination, where injury is driven by oligodendrocyte toxicity rather than adaptive immune responses, CD44 expression peaks within demyelinated regions of the CC during maximal myelin loss [14]. This suggests that CD44 upregulation reflects a reactive glial response to local tissue injury rather than systemic immune modulation. Similarly, Reinbach et al. reported strong CD44 induction in astrocytes and a subset of microglia during cuprizone demyelination, enriched in demyelinated white matter tracts, but with no effect on the extent of demyelination or gliosis upon deletion of CD44 [13]. Our results are consistent with the findings of Reinbach et al. [13], who reported a peak in CD44+ cells morphologically corresponding to activated astrocytes during demyelination, supporting the involvement of CD44 in the demyelination process. These observations are further corroborated by Bradford et al., who demonstrated a significant role for CD44 in reactive astrocytes [17]. Moreover, our data indicate a subsequent reduction in the number of CD44+ cells during remyelination, accompanied by morphological changes characterized by fewer cellular processes, which may be associated with a transition toward an inactivated astrocytic state.

Additional evidence from other CNS injury models reinforces this context-specific function. Ischemic stroke triggers a spatially restricted increase in CD44 expression within infarcted and peri-infarct regions, primarily in reactive astrocytes, neural stem/progenitor cells, and activated microglia/macrophages of both pro- and anti-inflammatory phenotypes [12]. Over time, CD44 expression becomes largely restricted to microglia/macrophages, marking long-term immune activation and tissue remodeling. Chronic hypoxia similarly induces persistent demyelination in the CC, with the greatest deficits observed in continuous hypoxia (CCH) mice, and likely corresponds to sites of elevated CD44 expression in astrocytes, microglia, and progenitor cells [18]. In both cases, persistent CD44 upregulation correlates with sustained white matter injury and impaired remyelination, suggesting that CD44 may contribute to a local environment that hinders oligodendrocyte regeneration and myelin repair [12, 18], which is consistent with our findings of dynamic changes in the number and morphology of CD44+ cells between de- and remyelination compared to healthy controls.

Despite these insights, several limitations should be considered. First, while our findings reveal significant alterations in the number of CD44+ cells across demyelination, remyelination, and control conditions, the direct mechanistic involvement of CD44 signaling in OPC maturation within the cuprizone model has yet to be established. Second, our analysis is limited to spatial and temporal expression patterns without functional manipulation of CD44 in vivo, which could clarify causality. Future studies should employ conditional knockouts or pharmacological modulation of CD44 in astrocytes, microglia, and progenitor populations to dissect its cell-type-specific contributions. Additionally, integration with transcriptomic or proteomic analyses could elucidate the downstream pathways through which CD44 influences glial activation, extracellular matrix remodeling, and remyelination.

CONCLUSION

In summary, our study demonstrates that CD44 is robustly upregulated in the CC during cuprizone-induced demyelination, with numbers peaking at 5 weeks of Cuprizone intoxication. Comparisons with autoimmune and ischemic models highlight the context-dependent functions of CD44, ranging from immune regulation to lesion-associated glial activation. These data support a model in which CD44 serves as a dynamic marker of injury-induced cellular responses and may modulate remyelination through its influence on glial and progenitor cell activity, providing a foundation for future mechanistic studies and potential therapeutic targeting.

animals used for scientific purposes and were approved by the Bulgarian Food Safety Agency (Approval Protocol No. 416/19.12.2024).

Data Availability Statement: *The raw data supporting the conclusions of this article will be made available by the authors upon request.*

Conflicts of Interest: *The authors declare no conflicts of interest.*

REFERENCES

1. Kipp M, Nyamoya S, Hochstrasser T, Amor S. Multiple sclerosis animal models: a clinical and histopathological perspective. Brain Pathol, 2017, 27(2):123-137. doi: 10.1111/bpa.12454.

2. Seitaridou Y, Dimitrova M, Chamova T, et al. Cost-effectiveness of multiple sclerosis therapies – a literature review. Acta Medica Bulg, 2022, 49(4):69-80. doi: 10.2478/amb-2022-0046.

3. Hauser SL, Aubert C, Burks JS, et al. Analysis of human T-lymphotrophic virus sequences in multiple sclerosis tissue. Nature, 1986, 322(6075):176-7. doi: 10.1038/322176a0.

4. Matsushima GK, Morell P. The neurotoxicant, cuprizone, as a model to study demyelination and remyelination in the central nervous system. Brain Pathol, 2001, 11(1):107-16. doi: 10.1111/j.1750-3639.2001.tb00385.x.

5. Ponta H, Sherman L, Herrlich PA. CD44: from adhesion molecules to signalling regulators. Nat Rev Mol Cell Biol, 2003, 4(1):33-45. doi: 10.1038/nrm1004.

6. Teder P, Vandivier RW, Jiang D, et al. Resolution of lung inflammation by CD44. Science, 2002, 296(5565):155-8. doi: 10.1126/science.1069659.

7. Dzwonek J, Wilczynski GM. CD44: molecular interactions, signaling and functions in the nervous system. Front Cell Neurosci, 2015, 9:175. doi: 10.3389/fncel.2015.00175.

8. Geloso MC, Ria F, Corvino V, Di Sante G. Expression of CD44 and its spliced variants: innate and inducible roles in nervous tissue cells and their environment. Int J Mol Sci, 2025, 26(17):8223. doi: 10.3390/ijms26178223.

9. Girgrah N, Letarte M, Becker LE, et al. Localization of the CD44 glycoprotein to fibrous astrocytes in normal white matter and to reactive astrocytes in active lesions in multiple sclerosis. J Neuropathol Exp Neurol, 1991, 50(6):779-92. doi: 10.1097/00005072-199111000-00009.

10. Back SA, Tuohy TM, Chen H, et al. Hyaluronan accumulates in demyelinated lesions and inhibits oligodendrocyte progenitor maturation. Nat Med, 2005, 11(9):966-72. doi: 10.1038/nm1279.

11. Naruse M, Shibasaki K, Yokoyama S, et al. Dynamic changes of CD44 expression from progenitors to subpopulations of astrocytes and neurons in developing cerebellum. PLoS One. 2013;8(1):e53109. doi: 10.1371/journal.pone.0053109.

12. Sawada R, Nakano-Doi A, Matsuyama T, et al. CD44 expression in stem cells and niche microglia/macrophages following ischemic stroke. Stem Cell Investig. 2020 Mar 10;7:4. doi: 10.21037/sci.2020.02.02.

13. Reinbach C, Stadler MS, Pröbstl N, et al. CD44 expression in the cuprizone model. Brain Res, 2020, 1745:146950. doi: 10.1016/j.brainres.2020.146950.

14. Flynn KM, Michaud M, Madri JA. CD44 deficiency contributes to enhanced experimental autoimmune encephalomyelitis: a role in immune cells and vascular cells of the blood-brain barrier. Am J Pathol. 2013 Apr;182(4):1322-36. doi: 10.1016/j.ajpath.2013.01.003.

15. Landzhov B, Gaydarski L, Stanchev S, et al. A Morphological and behavioral study of demyelination and remyelination in the cuprizone model: Insights into APLNR and NG2+ cell dynamics. Int J Mol Sci, 2024, 25(23):13011. doi: 10.3390/ijms252313011.

16. Paxinos G, Franklin K. The mouse brain in stereotaxic coordinates. 2nd ed. Academic Press. Cambridge, MA, USA, 2001, 55–63.

17. Bradford BM, Walmsley-Rowe L, Reynolds J, et al. Cell adhesion molecule CD44 is dispensable for reactive astrocyte activation during prion disease. Sci Rep, 2024, 14(1):13749. doi: 10.1038/s41598-024-63464-3.

18. Kanaan A, Farahani R, Douglas RM, et al. Effect of chronic continuous or intermittent hypoxia and reoxygenation on cerebral capillary density and myelination. Am J Physiol Regul Integr Comp Physiol, 2006, 290(4):R1105-14. doi: 10.1152/ajpregu.00535.2005.